Investigation of Mechanical Cardiorespiratory Interactions through Combined Structural and Functional Modelling

M Guerrisi[1], I Vannucci[1], T Karaja[2], N Toschi[1]

[1]Universitá degli Studi di Roma "Tor Vergata", Rome, Italy
[2]University of Tirana, Tirana, Albania

Abstract

Mechanical interplay between the adjacent ventricles is one of the principal modulators of physiopathological heart function, and the underlying mechanisms of interaction are only partially understood. In order to characterize the influence of chamber geometry on ventricular coupling, the ventricles and septum are modeled as portions of ellipsoidal shells, and configuration is derived as a function of pressure gradients. Diastolic volume (v) surfaces are calculated as a function of pressure (p), contralateral pressure (clp) and intrathoracic pressure (pt) and match literature data where available. Ventricular interaction is characterized in terms of partial derivatives in v-p-clp-pt space both under physiological and simulated pathological conditions. Inclusion of such interaction coefficients in a lumped parameter model of the circulatory system allows haemodynamic analysis of ventricular interplay in a variety of physiopathological circumstances.

1. Introduction

Ventricular interaction (VI) is involved in regulation and dys-regulation of cardiac functionality, and the asymmetry of interaction has been demonstrated. Several investigations point to the existence of a direct and global structural interaction between all cardiac walls [1]. Also, pericardial restraint acts as an important amplifier of VI, and mechanical ventilation studies as well as cine-MRI acquisition [2] have highlighted a significant modulation of VI by respiration. Numerous cardiovascular pathologies (e.g. ischemic heart disease, ventricular hypertrophy and congestive heart failure) frequently result in altered myocardial compliance, which in turn has been shown to modulate VI [3]. Numerous studies estimated wall stresses approximating ventricular shape as spherical, elliptical, cylindrical, or conical, however neglecting shear stresses and stress variations across thickness. All these studies consider the myocardium linear and isotropic. VI is often quantified in terms of coupling indexes between perturbations in state variables such as pl, pr, vl and vr, both in experimental [4] and model [5] studies. In most cases however the controlled perturbation will induce uncontrolled changes in all other variables, and the operating point of the system is not usually reported completely. In this study, we develop a 3D model of ventricular chambers [6] which accounts for trans-septal coupling, pericardial constraint, overall chamber deformation and respiration and seek to characterize VI in terms of coupling coefficients in v-p-clp-pt space, with the aim of studying its haemodynamic consequences through lumped-parameter modelling of the cardiovascular system.

2. Methods

Heart model

The LV, RV and the septum (SEP) are described as portions of thick-walled ellipsoidal shells, joined at the sulcus and surrounded by a pericardial membrane (PC). Material properties are described by a non-linear, non isotropic constitutive law [7] (Fig. 1). Shells have semi-axes b_i, a_i and c_i, are centered on (d_i, *0, 0)* and their middle surfaces are parameterized as ellipsoids:

$$S_i(a_i,b_i,c_i,\alpha_i,\beta_i) = \mathbf{r}_i; i = \{l,r,s\} \quad (1)$$

where α and β are local curvilinear coordinates. Total strain energy is:

$$W_{ij} = \kappa_{ij} \frac{e_{ij}^2}{(\rho_{ij} - e_{ij})^{\lambda_{ij}}} \quad , \quad W = W_{11} + W_{22} + W_{33} + W_{12} + W_{13} + W_{23} \quad (2)$$

where ρ (limiting strain), κ (scale factor) and λ (curvature parameter) are material parameters, e_{ij} is strain and the subscripts *i, j* represent coordinate directions (α*=1,* β*=2, w=3*). Pericardial material properties are also described by Eqn. (2). We then have $\sigma_{ij}(e) = \partial W_{ij} / \partial e_{ij}$. Requiring static equilibrium of a shell element results in [8]:

$$\frac{\partial \mathbf{T}^{(1)}}{\partial \alpha}\mathrm{d}\alpha + \frac{\partial \mathbf{T}^{(2)}}{\partial \beta}\mathrm{d}\beta + \mathbf{p}AB\mathrm{d}\alpha\,\mathrm{d}\beta = 0$$
$$\frac{\partial \mathbf{M}^{(1)}}{\partial \alpha}\mathrm{d}\alpha + \frac{\partial \mathbf{M}^{(2)}}{\partial \beta}\mathrm{d}\beta + A\mathrm{d}\alpha\left(\mathbf{e}_1 \times \mathbf{T}^{(1)}\right) + B\mathrm{d}\beta\left(\mathbf{e}_2 \times \mathbf{T}^{(2)}\right) = 0 \qquad (3)$$

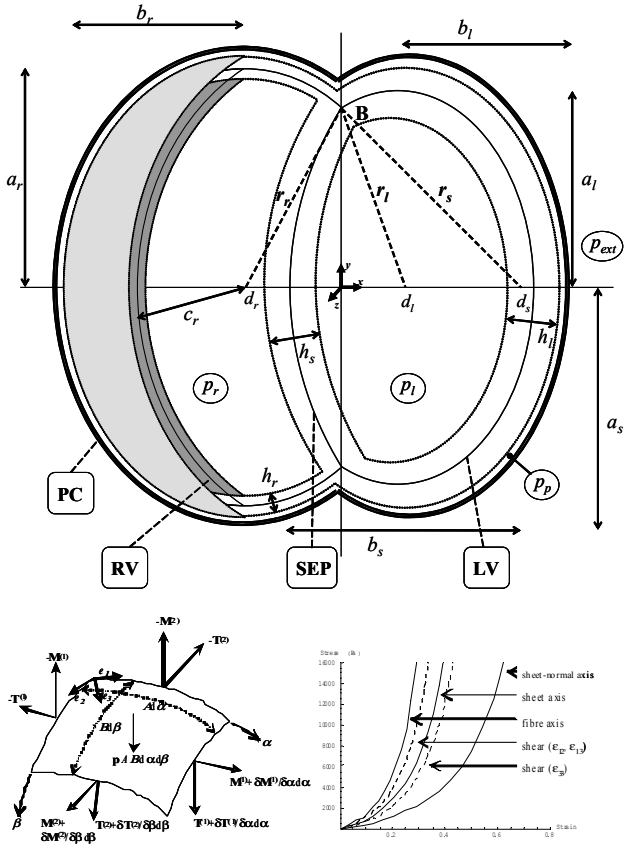

Figure 1. Model Geometry, shell element and myocardial constitutive law

where (A,B) are Lamé parameters derived from the first and second fundamental form of surfaces. Further, the differential element is acted upon by an external surface load of intensity $\mathbf{p} = p_1\mathbf{e}_1 + p_2\mathbf{e}_2 + p_3\mathbf{e}_3 = \Delta p\mathbf{e}_3$. Shells are constrained to displace coherently at the sulcus (**B**):

$$\mathbf{r}_r^* - \mathbf{r}_r = \mathbf{r}_s^* - \mathbf{r}_s = \mathbf{r}_l^* - \mathbf{r}_l \qquad (4)$$

with additional force and moment boundary conditions:

$$\mathbf{T}_l^{(1)*} + \mathbf{T}_r^{(1)*} + \mathbf{T}_s^{(1)*} = 0$$
$$\mathbf{M}_l^{(1)*} + \mathbf{M}_r^{(1)*} + \mathbf{M}_s^{(1)*} = 0$$

Circulation model

A lumped-parameter model of the entire circulatory system (Fig. 2) was previously developed which accounts explicitely for every compartment of systemic and pulmonary circulation as well as nonlinear behaviour of aortic and peripheral circulation. Structure of the model and parameter values were derived through extensive literature survey. Ventricular pressure-volume waveforms match literature data where available.

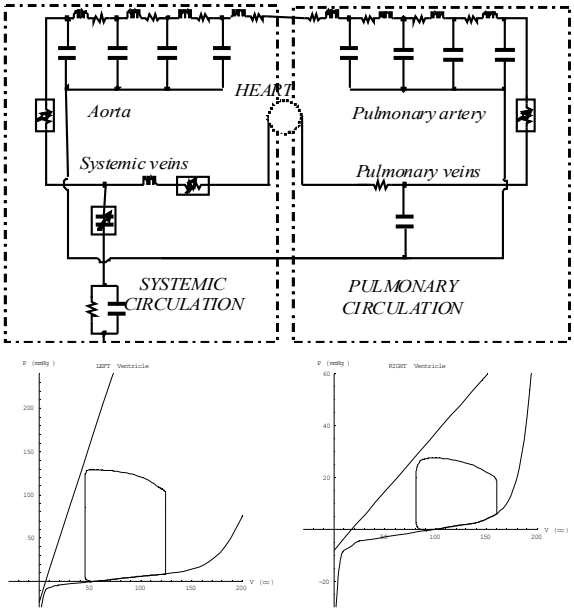

Figure 2. Circulation Model and ventricular p-v loops.

3. Results

Principal strains as a function of pressure/volume

Heart model parameterisation is obtained from the literature. As validation, the model was inflated to p_l =120 mmHg (0.1 mmHg steps, p_r = 4.5 mmHg, p_t = 0 mmHg). Resulting principal stresses and strains in the equatorial region of the middle surface were are shown in Fig. 3 (top) as a function of p_l.This allows comparison

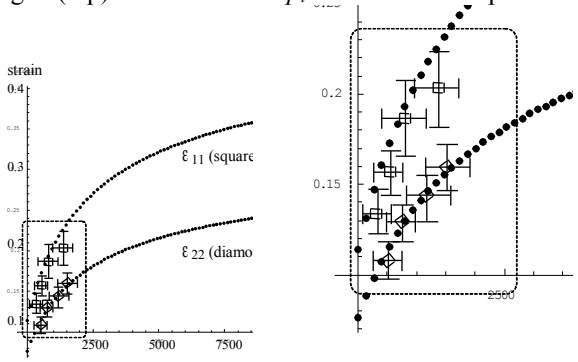

Figure 3. Principal strains vs p_l

with the experimental results in (9) (squares and

diamonds). Calculated strains are in good agreement with experimental data in the region covered by the experimental study, which is on the low end of the physiological range (0-2 kPa).

Ventricular Interaction

A system of 5 interrelated variables allows for 20 non-trivial partial derivatives (i.e. coupling coefficients). Fig. 4 shows reference values of pressure-pressure coupling coefficients as a function of p_l and p_r, evaluated at p_t = -8 mmHg (inspiration), p_t = -4 mmHg (average) and p_t = 4 mmHg (expiration).

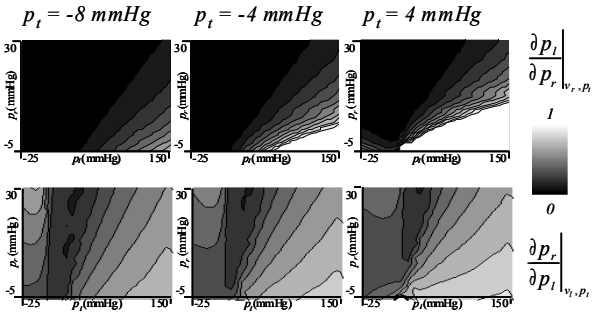

Figure 4. Baseline *p-p* interaction coefficients

Several cardiovascular pathologies can be well represented well by altering myocardial or pericardial material properties. Figs. 5-8 show values of coupling coefficient variations with respect to baseline (Fig. 4), plotted in percentages as a function of p_l and p_r (contour plots).

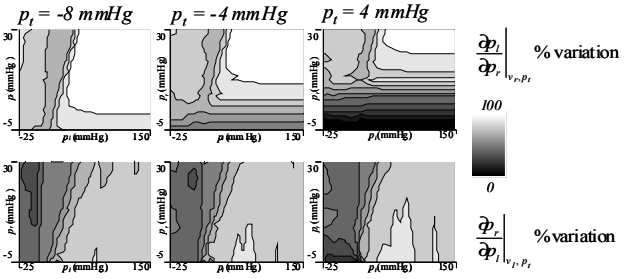

Figure 5. Constrictive Pericarditis

A stiffer pericardium (constrictive pericarditis - CP) always enhances ventricular coupling. The coupling is raised by up to 100% of reference value, and this effect is seen particularly in regions of high p_l and high p_r. Some aspects of this effect are reported in literature (10). The effects are greater in the R→L direction than in the opposite direction. Further, a lower p_t (inspiration) enhances the effect of pericardial constraint, while a higher p_t mitigates it.

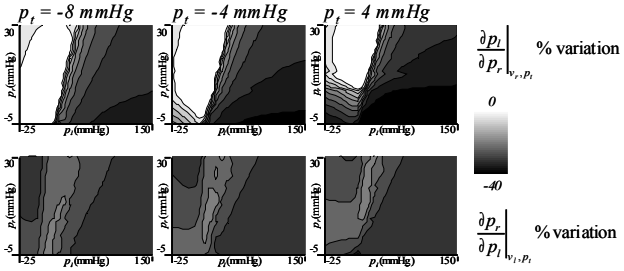

Figure 6. Restrictive Cardiomyopathy

A globally stiffer myocardium (restrictive cardiomyopathy - RCMP, LV, RV and SEP) always leads to diminished ventricular interaction, confirming experimental observations (2). The coupling is diminished by up to 40% of reference value, particularly in regions of high p_l and low p_r The effects of a stiffened myocardium are greater in the R →L direction. Further, a lower p_t (inspiration) decreases the effect of myocardial stiffening, while a higher p_t (expiration) enhances it.

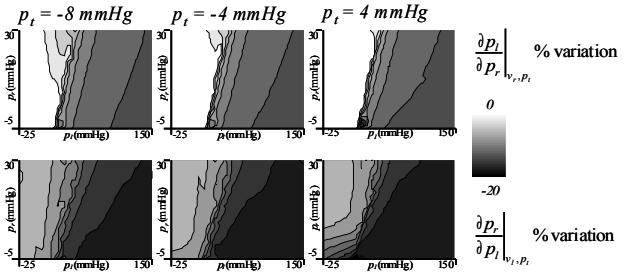

Figure 7. Left ventricular and septal hypertrophy

Augmenting LV and SEP thickness (left ventricular and septal hypertrophy - LVSH) always reduces ventricular interaction as previously observed experimentally (11). The coupling is diminished by up to 20% of the reference value, and this effect is seen particularly in regions of high p_l and low p_r. The effects of a thicker LV and SEP are greater in the L →R direction than in the opposite direction. Further, a lower p_t (inspiration) slightly decreases, a higher p_t slightly increases the effect of LVH.

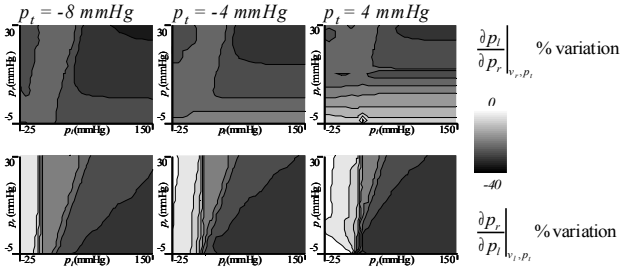

Figure 8. Left dilatative cardiomyopathy

Left dilatative cardiomyopathy (LDCMP): Ventricular interaction is always reduced in this case. The coupling is diminished by up to 40% of the reference values,

particularly in the L →R direction. Further, A lower p_t (inspiration) enhances this effect (especially in the R →L direction), and expiration mitigates it.

Effect on p-v relationships

Fig. 9 shows *p-v* histories for both chambers both in baseline conditions and under the altered material parameter conditions described above. We expect an alteration in the system to affect both chambers in virtue of ventricular interaction. In these particular realizations, all conditions but LDCMP cause a leftward/upward shift in both R and L p-v curves, while LDCMP renders the LV more compliant and, by virtue of VI, this effect is seen to a lesser extent in the RV also.

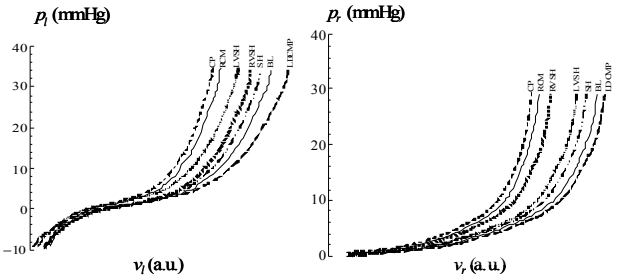

Figure 9. A/B: Calculated p-v relationships for LV (A) and RV (B) for baseline conditions (BL), contrictive pericarditis (CP), restrictive cardiomyopathy (RCM), left ventricular and septal hypertrophy (LVSH), right ventricular and septal hypertrophy (RVSH), septal hypertrophy (SH) and left dilatative cardiomypathy (LDCMP).

4. Discussion and conclusions

We analytically isolate effects of a fluctuation of one variable on another variable, hence requiring care when comparing coefficients to experimental measurements, where this filtering is never possible. Overall, we are able to reproduce the mode (existence and extent) and direction (signs of coefficients) of VI in all pairs of variables analysed and, where available, experimental data fits well with our results. Interaction mechanisms appear to be profoundly asymmetrical, to an extent which could lead to postulate different combined mechanisms of pressure transmission in the two directions (e.g. L →R interaction mediated more through the septum, while R →L dominated by overall chamber deformation effects aided by pericardial constraint). Further, it appears that respiration is generally more coupled to the RV, possibly acting on the LV through the RV.

We validate a VI model which is accurate from a material description and mechanical point of view. It provides more complete insight into the way cardiac chambers influence each other, and can be employed for quantitative characterisation and predictions of VI where experimental studies cannot reach. We demonstrate its applicability to circumstances of pathological alterations in myocardial properties, and in particular to the prediction of the effect of the latter on VI, which can be quantified using echocardiography or cine-MRI techniques

Acknowledgements

Con il contributo del Ministero degli Affari Esteri, Direzione Generale per la Promozione e la Cooperazione Culturale.

References

[1] Yamaguchi S, Tsuiki K, Miyawaki H, Tamada Y, Ohta I, Sukekawa H, et al. Effect of left ventricular volume on right ventricular end-systolic pressure-volume relation. Resetting of regional preload in right ventricular free wall. Circ Res 1989 Sep;65(3):623-31.

[2] Francone M, Dymarkowski S, Kalantzi M, Rademakers FE, Bogaert J. Assessment of ventricular coupling with real-time cine MRI and its value to differentiate constrictive pericarditis from restrictive cardiomyopathy. Eur Radiol 2006 Apr;16(4):944-51.

[3] Farrar DJ, Chow E, Brown CD. Isolated systolic and diastolic ventricular interactions in pacing-induced dilated cardiomyopathy and effects of volume loading and pericardium. Circulation 1995 Sep 1;92(5):1284-90.

[4] Santamore WP, Bartlett R, Van Buren SJ, Dowd MK, Kutcher MA. Ventricular coupling in constrictive pericarditis. Circulation 1986 Sep;74(3):597-602.

[5] Chung DC, Niranjan SC, Clark JW, Jr., Bidani A, Johnston WE, Zwischenberger JB, et al. A dynamic model of ventricular interaction and pericardial influence. Am J Physiol 1997 Jun;272(6 Pt 2):H2942-H2962.

[6] Toschi N, Guerrisi M. Interventricular coupling coefficients in a thick shell model of passive cardiac chamber deformation. Med.Biol.Eng.Comput. 2008.

[7] Nash MP, Hunter PJ. Computational Mechanics of the Heart. J Elast 2000;61:113-41.

[8] Ventsel E, Krauthammer T. Thin Plates & Shells: Theory, Analysis, & Applications. New York/Basel: CRC; 2001.

[9] Omens JH, May KD, McCulloch AD. Transmural distribution of three-dimensional strain in the isolated arrested canine left ventricle. Am J Physiol 1991 Sep;261(3 Pt 2):H918-H928.

[10] Spadaro J, Bing OH, Gaasch WH, Weintraub RM. Pericardial modulation of right and left ventricular diastolic interaction. Circ Res 1981 Feb;48(2):233-8.

[11] Slinker BK, Chagas AC, Glantz SA. Chronic pressure overload hypertrophy decreases direct ventricular interaction. Am J Physiol 1987 Aug;253(2):H347-H357.

Maria Guerrisi, Fisica Medica, ed. H, Facoltá di Medicina e Chirurgia, Universitá degli Studi di Roma “Tor Vergata”, Via Montpellier 1 - 00133 Rome, Italy guerrisi@med.uniroma2.it